Progress In Electromagnetics Research B, Vol. 58, 71–82, 2014

A Compact Diplexer Based on Low Profile Multilayer FSS Filters for Ultra-High Data Rate Point to Point Wireless Communication System

Tao Zhang and Habiba Hafdallah Ouslimani*

Abstract—In this paper, we propose the design of multilayer frequency selective surfaces (FSS) waveguide band-pass filters (WBPF). The WBPFs are designed to operate at two different frequency channels, respectively 71–76 GHz (Rx) and 81–86 GHz (Tx). The cross section surface of the FSS is imposed by the WR12 waveguide rectangular section's dimensions. The WBPFs are inserted symmetrically in a T-junction waveguide to design a compact diplexer. This is a basic component developed for an efficient integration in the future E-band millimeter-wave transceiver. The multilayer FSS structure uses only non-resonant sub-wavelength unit cell elements; metallic patch and slot. To reach high channel isolation (≈ 70 dB) a seven order filter was required. Hence, each filter is composed of 13 capacitive and inductive metallic FSS spaced by 12 ultra-thin dielectric substrate layers. The dielectric material is Rogers Ultralam 3850 (Liquid Crystalline Polymer; LCP circuit material). The filter's overall thickness is $< \lambda/4$. The numerical studies have been performed using finite element method simulator (HFSS) and CST Studio Suites Tools. The experimental validation has been also done in the X band frequency by developing a fifth order FSS WBPF. Good agreements between simulated and measured results are obtained.

1. INTRODUCTION

The millimeter wave domain is very important for high capacity and high speed wireless communication systems. In recent years, the 71–76 and 81–86 GHz frequency bands (widely known as "E band") are respectively allocated by the FCC and the ETSI for Gigabit wireless communications system applications. The E-band technology can provide solutions for backhaul of 4G, WiMAX, LTE, etc.

This study is done under the project "E-band for high bit rate digital links" ELHAN of the SYSTEMATIC French cluster [1]. The main goal of this project is to enable the capability to get low-cost high-bit rate (> 1G bits/s), high spectrum efficiency (> 7 bits/s/Hz), and short range (< 4 km) point to point radio links on the newly worldwide standardized E band by developing the basic components and technologies needed for this purpose. The scientific innovations of RF part concern the definition and design of a new kind of high-efficiency low-cost antennas and diplexers. We focus on the design of a new diplexer at E-band frequency range suitable for the application to the antenna array system. In order to meet the specifications of "ELHAN" project, a compact, light weight, high isolated diplexer should be designed.

The diplexers are generally designed using standard metallic waveguide filters, metallic cavity or planar technology [2–4]. Such structures have the disadvantage of being too thick (bulky), heavy, expensive, and difficult to integrate systems in millimeter band [5–7].

Received 21 December 2013, Accepted 13 January 2014, Scheduled 20 January 2014

* Corresponding author: Habiba Hafdallah-Ouslimani (habiba.ouslimani@u-paris10.fr).
The authors are with the Energetic Mechanic Electromagnetic Lab, LEME-4416, Waves Material System Group (OMS), University Paris Ouest Nanterre La Défense, 50 rue de Sèvres, Ville d'Avray 92410, France.

The traditional FSSs are considered as spatial filters (low pass, high pass band-stop and band-pass [8]) and can be applied, for example, to the design of Radom for antennas and dichroic sub-reflector for parabolic Cassegrain antenna systems [9]. They are constituted of bi-dimensional periodic array of metallic structures printed on or not on dielectric substrates. High order band-pass filters should be used in order to obtain high isolation between diplexer channels and a high level of rejection of out band. The standard structures often use several (N) first-order FSS filters, putting them in cascade. The distance between two FSSs is quarter wavelength $\lambda/4$ (λ is the free-space wavelength of the pass-band center frequency) [9]. For our application, this solution gives rise to thick and bulky structures not suitable for designing a high performance and compact diplexer.

In recent years, a new class of FSS with low-profile feature is intensively studied, as it is reported by the authors in [10–15]. This class of FSS structure is studied and realized at X-band frequency range. The overall thickness of a third-order band-pass new FSS filter can reach $\lambda/24$ (λ is the free-space wavelength of band-pass central frequency) in [15]. Due to their lightweight and thin thickness properties, this class of FSS is very suitable for designing high performance compact diplexer.

In this paper, we develop a new compact waveguide diplexer using low-profile multilayer FSS waveguide band-pass filters (FSS-WBPF) in E-band frequency range with a high channel isolation $\approx 70\,\text{dB}$. The proposed WR12 waveguide based diplexer can be applied to the antenna array system of an E-band ultra-high data rate point-to-point radio link. Duo to the manufacturing difficulties and the fabrication accuracy requirements at millimeter wave domain, the designed FSS-WBPFs use the ultra-thin Liquid Crystalline Polymer (LCP) circuit material (Rogers Ultralam 3850) with a thickness of 0.1 mm, relative permittivity $\varepsilon_r = 3.87$ and loss tangent $\tan(\delta) = 0.0025$. The used seventh order FSS-WBPFs have an overall thickness of $\approx \lambda/4$ (λ is the free-space wavelength of band-pass central frequency). For the purpose of experimental investigation, a fifth-order WR90 waveguide band-pass filter with a bandwidth of $\approx 5\%$ (9.75–10.25 GHz) is fabricated and measured. In order to satisfy the high fabrication accuracy requirement at 80 GHz, we develop a simplified design process to achieve the desired results by using basic shape (square) for the FSS unit cells. The measurement result of fabricated prototype confirms the process by an excellent agreement with numerical result.

2. DIPLEXER TOPOLOGY

The proposed FSS-based waveguide diplexer is given in Fig. 1(a). It consists of a T-junction WR12 E-band waveguide with symmetrically inserted filters, one in each branch. The dimensions of the WR12 rectangular waveguide cross section are $3.0988 \times 1.5494\,\text{mm}^2$. The designed WBPFs frequency channels are 71–76 GHz and 81–86 GHz.

The topology of the filters and the details of the multilayer FSS structure are shown in Fig. 1(b). Each seven order filter is composed of 13 capacitive and inductive FSS separated by 12 ultra-thin dielectric substrate layers. All of those components are stacked using specific bonding technique. The FSS filter begins and ends with capacitive metallic layers. The FSS layers with odd number are always capacitive while those with even number are always inductive. Fig. 1(b) gives the three-dimensional (3D) details of stacked multilayer FSS WBPF (cascading method and bonding technique).

In HFSS model, the FSS structure is vertically inserted into a rectangular waveguide. The boundary conditions are imposed by the metallic structure of the guide. Therefore, the actual design is different from that of the free-space type with infinite size described in [8] which requires periodicity conditions (with two sets of vertical master-slave borders). The full-wave EM simulations (FEM HFSS simulator) use a perfect electric conductors; PEC boundary for the four waveguide sidewalls of FSS waveguide filter structure (4 sides). Fig. 1(c) gives the HFSS simulation model setup where the filter is defined by two orthogonal sets of PEC boundary conditions.

3. FSS WAVEGUIDE FILTER DESIGN METHOD

3.1. Equivalent Circuit Approach

The FSS-WBPF is designed using lumped equivalent circuit approach. Different steps, as described by Fig. 2, were necessary.

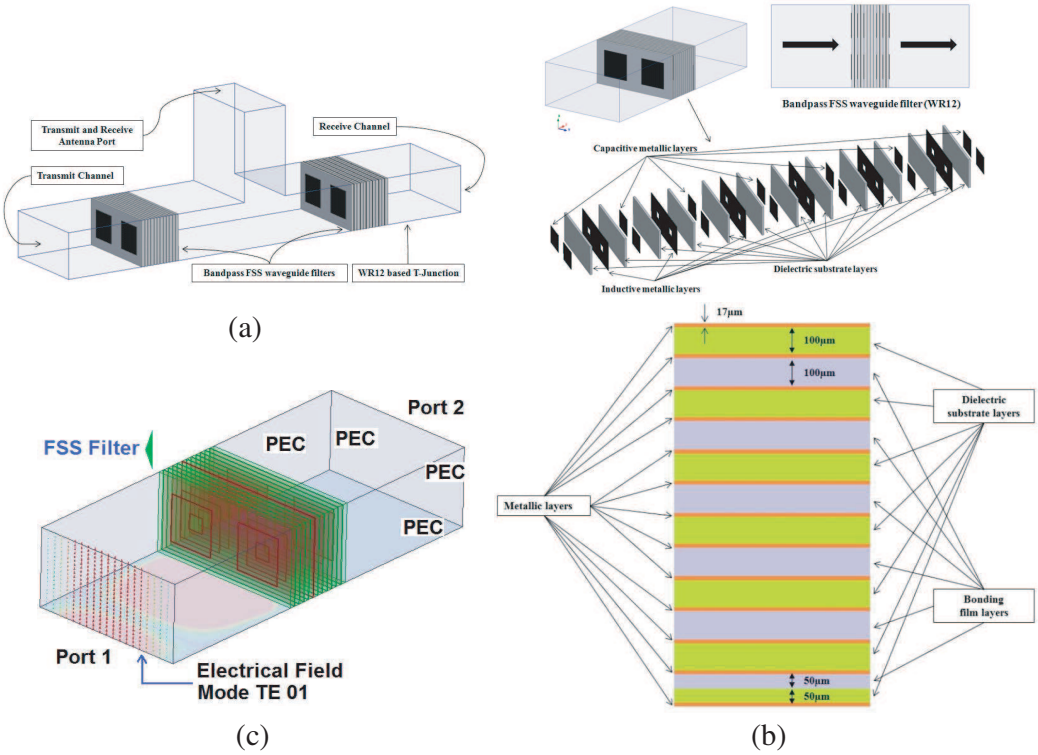

Figure 1. (a) Topology of proposed E-band waveguide diplexer (WR12) composed of a couple of multilayer FSS band pass filters (FSS-WBPF). (b) Stacked layers (cascading method and bonding technique). The dielectric material is Rogers Ultralam 3850, the bonding film used is Rogers Ultralam 3908. (c) Rectangular waveguide multilayer FSS band-pass filter's HFSS Model setup.

- Firstly, a conventional lumped circuit model shown is established [16, 17] for the seventh order band-pass filter (Fig. 2(a)). Table 1 gives the normalized parameters. Here we choose a filter with a "Tchebychev" frequency response and a ripple of 0.1 dB. The filter's bandwidths are respectively from 71 to 76 GHz and 81 to 86 GHz which corresponds to a 5 GHz band for each channel.
- Secondly, based on the circuit model of Fig. 2(a), admittance inverter transformation (Fig. 2(b)) and resonant LC series-parallels conversion are performed following the method reported in [12, 13]. The obtained equivalent circuit is given by Fig. 2(c).
- Finally, the equivalent circuit, shown by Fig. 2(d) is obtained using "Π" to "T" circuit equivalence [12, 13].

Table 1. Normalized parameter values of seventh order "Tchebychev" bandpass filter with a ripple of 0.1 dB.

Order (n)	$g_0 = g_8$	$g_1 = g_7$	$g_2 = g_6$	$g_3 = g_5$	g_4
7	1	1.1811	1.4228	2.0966	1.5733

First channel: Fig. 2(a)

$C_1 = C_7$	$C_2 = C_6$	$C_3 = C_5$	C_4
99.72 fF	0.275 fF	117.0 fF	0.249 fF
$L_1 = L_7$	$L_2 = L_6$	$L_3 = L_5$	L_4
0.047 nH	17.07 nH	0.027 nH	18.88 nH

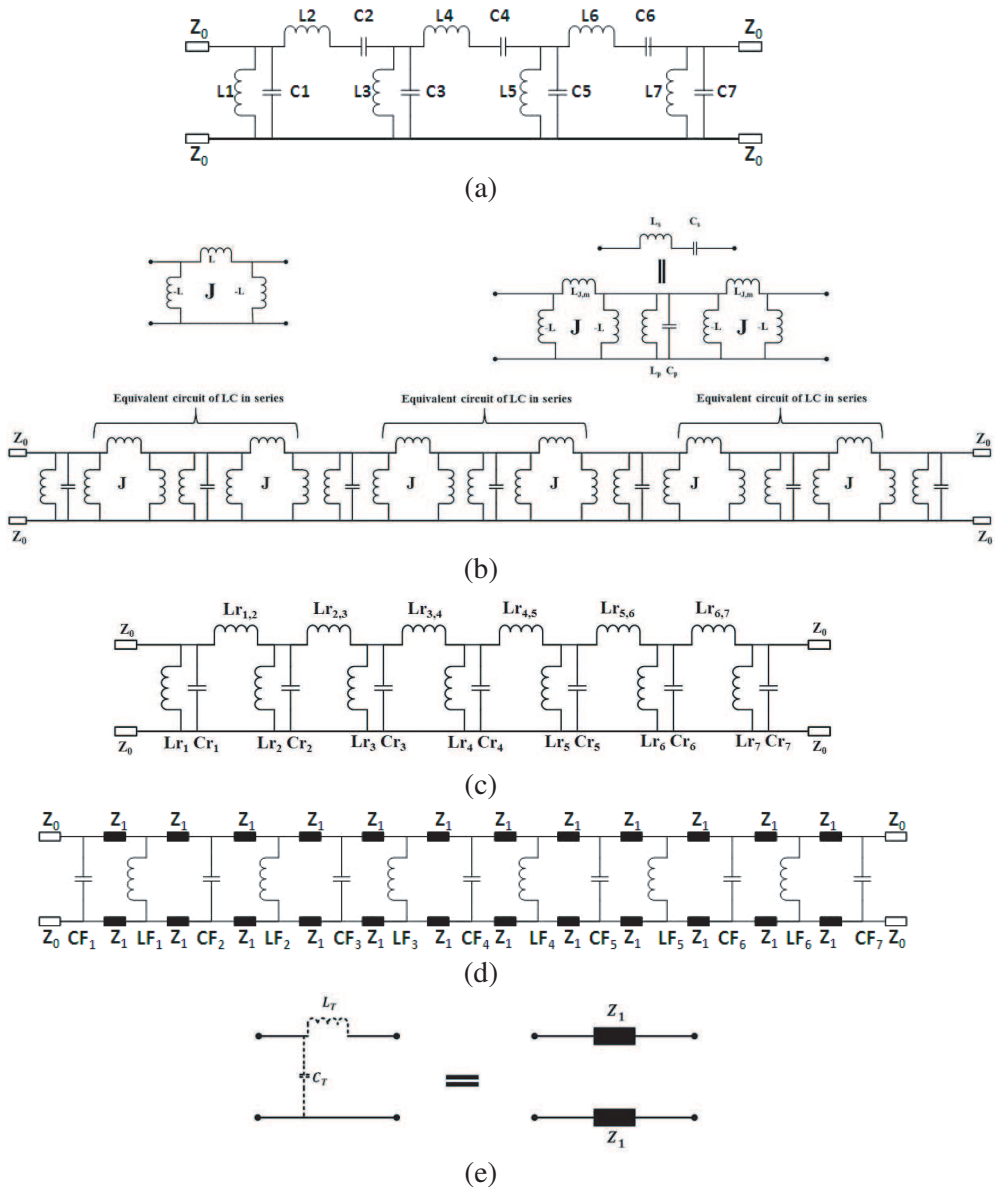

Figure 2. (a) Conventional lumped circuit model of seventh order bandpass filter, (b) "J" Admittance inverter transformation. (c) Equivalent circuit obtained after admittance inverter transformation. (d) Final equivalent circuit model of seventh order band pass filter. (e) Transmission line model of the dielectric substrate layers and its equivalent lumped circuit.

- The dielectric substrate layers are described in this final circuit using transmission line model with a characteristic impedance Z_1 given by (1) and (2) and a height h approximately given by formula (3). The transmission line's lumped equivalent circuit is depicted by Fig. 2(e) [12].

$$Z_1 = \frac{L_T}{C_T} \tag{1}$$

$$Z_1 = \frac{Z_0}{\sqrt{\varepsilon_r}} \tag{2}$$

$$h_{dielectric\ layer} = \frac{L_T}{\mu_0 \mu_r} \tag{3}$$

To achieve a uniform height for all the dielectric substrate layers, full-wave optimization should be performed again. The free-space characteristic impedance $Z_0 = 377\,\Omega$ transmission lines at the two ends (Fig. 2) correspond to the semi-infinite space. In the final model (Fig. 2(d)), the lumped equivalent elements, parallel inductors ($LF_1, LF_2, \ldots, LF_6$) and parallel capacitors ($CF_1, CF_2, \ldots, CF_7$) are calculated using a developed MATLAB program.

3.2. Capacitive and Inductive FSS Design

As described above, the FSS WBPFs are obtained by cascading respectively capacitive and inductive metallic layers spaced by dielectric substrates. The FSS capacitive pattern is designed with metallic periodic patches shown in Fig. 3(a). The inductive layer is designed with periodic square metallic slots shown in Fig. 3(b). FSS structures are designed for vertical polarization (TE01 fundamental mode of the waveguide, Fig. 1(c)). For these reasons, the most appropriate shapes are squares and rectangles patches.

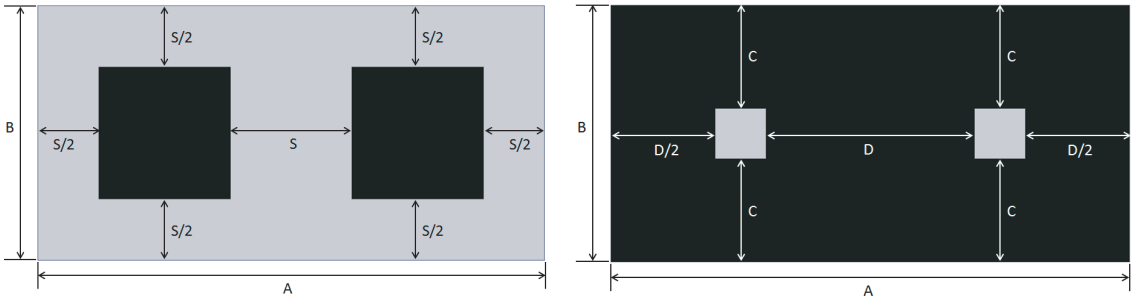

Figure 3. Capacitive and inductive unit cells with dimensions of WR12 waveguide. (a) Unit cell of capacitive layers. (b) Unit cell of inductive layers.

Optimizing the size of the square metallic patches and slots, as well as the height of the dielectric substrate layers, allow to control the values of L and C elements in the final equivalent circuit [18, 19]. Indeed, from the recent publications in this area, it is remarkable to note the possibility of calculating the values of the final passive lumped elements of FSS filter electric model using the geometrical dimensions of the unit cells and vice versa. Therefore, it is possible to go back to the basic geometrical dimensions of the unit cells of the FSS filter from the final equivalent circuit model. We can determine approximately the geometries of the capacitive and inductive unit cells using the calculated lumped element values (parallel capacitors and parallel inductors). The formulas (4) and (5) give the relations between the values of lumped elements and the geometry of the physical FSS metallic patterns [19].

$$C_{parallel} = \varepsilon_0 \varepsilon_{eff} \left(\frac{2B}{\pi}\right) \ln\left(\frac{1}{\sin\left(\frac{\pi S}{2B}\right)}\right) \tag{4}$$

$$L_{parallel} = \mu_0 \mu_{eff} \left(\frac{B}{2\pi}\right) \ln\left(\frac{1}{\sin\left(\frac{\pi C}{B}\right)}\right) \tag{5}$$

3.3. Numerical Simulation Results

Table 2 summarizes the optimized lumped element values; $CF_1, CF_2, \ldots, CF_7$ and $LF_1, LF_2, \ldots, LF_6$ and the dimensions of the optimized FSS unit cells.

The FSS WBPFs are excited with the TE10 fundamental wave guide mode (Fig. 1(c)). The transmission and reflection coefficients are studied from 55 GHz to 100 GHz. A dielectric loss tangent of $\tan(\delta) = 0$ is taken for the first simulations. Fig. 4 presents the obtained simulated frequency responses. Very high channel isolation and high rejection of out of band are observed. The reflection

Table 2. Element values of equivalent circuit models and FSS waveguide band-pass filter dimensions.

Z_0	Z_1	h (mm)	ε_r	A	B	Order
377 Ω	191.6 Ω	0.1 mm	3.87	3.098 mm	1.549 mm	7

Band 1: 71–76 GHz

$C_1 = C_7$	$C_2 = C_6$	$C_3 = C_5$	C_4
99.72 fF	0.275 fF	117.0 fF	0.249 fF
$L_1 = L_7$	$L_2 = L_6$	$L_3 = L_5$	L_4
0.047 nH	17.07 nH	0.027 nH	18.88 nH

$CF_1 = CF_7$	CF_2 to CF_6	LF_1 to LF_7
0.033 pF	0.066 pF	0.011 nH

$S_1 = S_7$	S_2 to S_6	C	D
0.623 mm	0.64 mm	0.623 mm	1.246 mm

Band 2: 81–86 GHz

$C_1 = C_7$	$C_2 = C_6$	$C_3 = C_5$	C_4
99.72 fF	0.213 fF	117.0 fF	0.193 fF
$L_1 = L_7$	$L_2 = L_6$	$L_3 = L_5$	L_4
0.036 nH	17.07 nH	0.021 nH	18.88 nH

$CF_1 = CF_7$	$CF_2 = CF_6$	$CF_3 = CF_5$	CF_4	LF_1 to LF_6
0.0255 pF	0.051 pF	0.051 pF	0.051 pF	0.01 nH
S_1 to S_7	S_2 to S_6	C	D	
0.745 mm	0.763 mm	0.637 mm	1.274 mm	

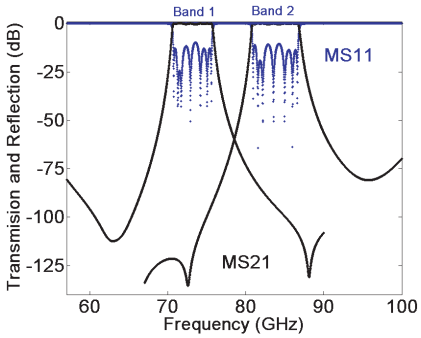

Figure 4. Simulated transmission and reflection coefficients of the designed FSS waveguide band-pass filters for the two channels; 71–76 GHz and 81–86 GHz (using HFSS simulator).

coefficient magnitude (S_{11} (dB)) is below −15 dB over the whole bandwidths which indicate very good matching impedance of the FSS filters. The transmission is perfect with any insertion loss inside the two bandwidths.

Figure 5 shows the magnitude of the distributed electric field through the filters for some characteristic frequencies (70, 73.5, 77, 80, 83.5, and 87 GHz). Fig. 5(a) and Fig. 5(b) are obtained at the two central frequencies, respectively 73.5 GHz and 83.5 GHz, and a very good electric field transmission is observed. In contrast, any electrical field transmission is achieved for the other out of band frequencies (70, 77, 80, and 87 GHz) as shown respectively by Fig. 5(c) to Fig. 5(f).

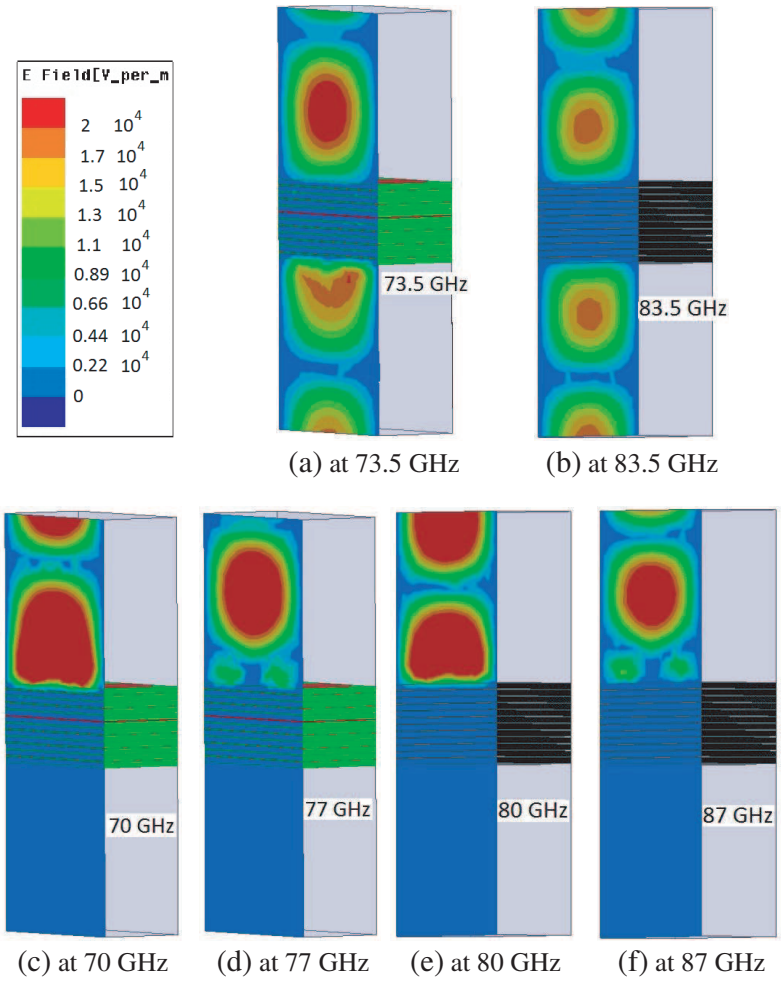

(a) at 73.5 GHz (b) at 83.5 GHz

(c) at 70 GHz (d) at 77 GHz (e) at 80 GHz (f) at 87 GHz

Figure 5. Total electric field magnitude through the FSS filter; (a) and (b) At different frequencies inside the band-pass domains at respectively 73.5 GHz and 83.5 GHz. (c) to (f) At frequencies located on the edges of the filter band-pass, respectively 70 GHz, 77 GHz, 80 GHz, and 87 GHz.

4. PARAMETRIC STUDIES

In the E-band frequency domain (mm-wavelength $\lambda_{-80\,\mathrm{GHz}} = 3.75\,\mathrm{mm}$), the request accuracy is around, or less than 10–50 micrometers. Hence, a very small variation of the physical parameters (geometrical dimensions and/or substrate properties) can lead to a very strong change of the designed multilayer FSS WBPFs frequency response. So, it is important to investigate the evolution of the frequency response according to the tolerances (known or supposed) on the physical parameters such as the relative dielectric permittivity ε_r and loss tangent $\tan(\delta)$.

4.1. Relative Dielectric Permittivity Sensitivity

The nominal value of the dielectric substrate relative permittivity is $\varepsilon_r = 3.87$. A tolerance error of about $\approx \pm 5\%$ ($\Delta\varepsilon_r = \pm 0.2$) is assumed and applied to the filters.

The simulation results for $\varepsilon_r = 3.67$ and $\varepsilon_r = 4.07$ are compared to those of $\varepsilon_r = 3.87$ and shown by Fig. 6(a) and Fig. 6(b) respectively for the two channel sub-bands. As shown by Fig. 6, when the dielectric permittivity increases 0.2 ($\varepsilon_r = 3.87 + 0.2$); the overall frequency responses (both transmission and reflection coefficients) shift toward lower frequency ($\approx -2.5\,\mathrm{GHz}$). In a same manner, when ε_r decreases by 0.2 ($\varepsilon_r = 3.87 - 0.2$), the frequency responses shift of about $\approx 2.5\,\mathrm{GHz}$ toward higher frequency. Far from the frequency domain of interest, the frequency responses of the filter are

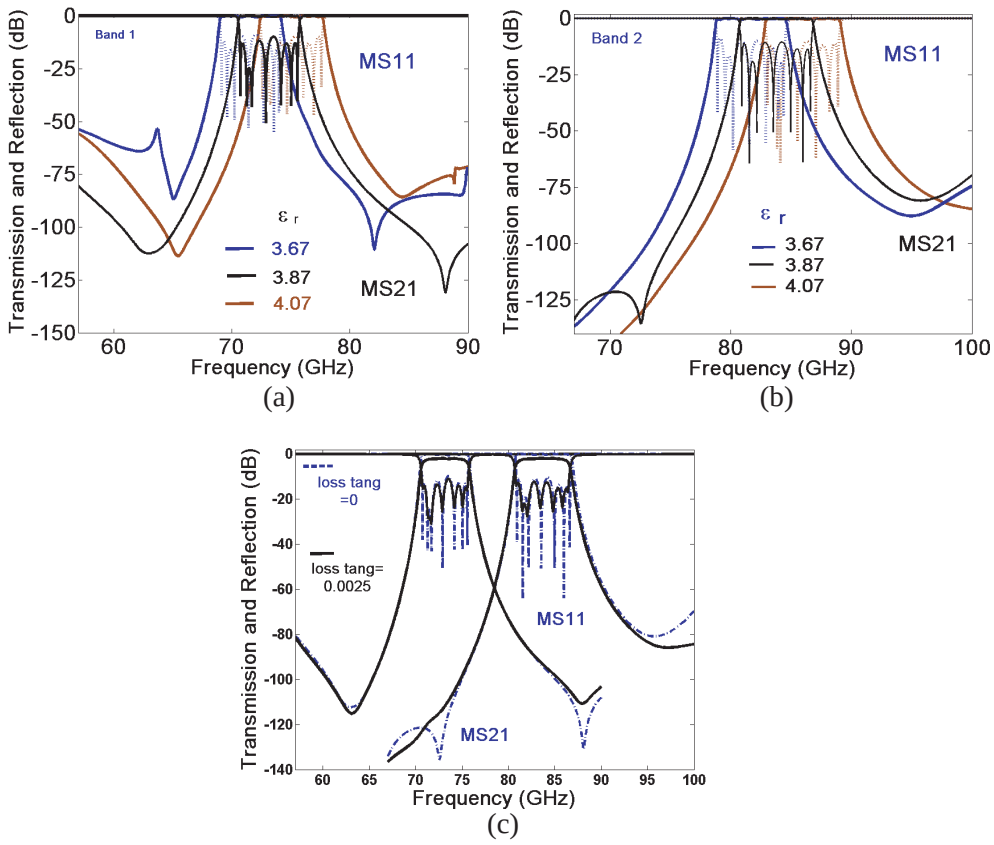

Figure 6. Parametric studies of FSS waveguide bandpass filters: (a) Relative dielectric permittivity sensitivity study: simulation results of two studied cases $\varepsilon_r = 3.67$ (Dashed grey line) and $\varepsilon_r = 4.07$ (Solid grey line) at frequency band 71–76 GHz. (b) Relative dielectric permittivity sensitivity study: simulation results of two studied cases $\varepsilon_r = 3.67$ (Dashed grey line) and $\varepsilon_r = 4.07$ (Solid grey line) at frequency band 81–86 GHz. (c) Dielectric loss tangent sensitivity study: transmission coefficient results of two studied cases $\tan(\delta) = 0$ (Dashed grey line) and $\tan(\delta) = 0.0025$ (Solid black line).

distorted. This dramatically deformation of the frequency behaviors demonstrate the importance of the dielectric substrate at this frequency scale.

4.2. Dielectric Loss Tangent Sensitivity

Only two cases are investigated: dielectric substrate without losses: $\tan(\delta) = 0$ and with losses $\tan(\delta) = 0.0025$ (nominal value given by the data sheet). Fig. 6(c) shows the simulated results (magnitude of the transmission and reflection coefficients). A transmission loss (insertion loss) of 2 dB is observed over the two bandwidths. The slopes of the response curves, their bandwidth, and the level of channel isolation are not significantly changed.

5. EXPERIMENTAL SETUP AND MEASUREMENT RESULTS

Figure 7 gives photographs of the FSS WBPFs prototypes, fabricated in the E-band domain by ELVIA (Cherbourg France). Experimental measurements have not been made, since no measurement facilities in the mm-wave frequency range have been available in our laboratory. Since we have X-band instrumentation facilities, the experimental validations are done around 10 GHz by developing a fifth order FSS waveguide band-pass filter. Same procedure and design methodology (presented earlier) are used.

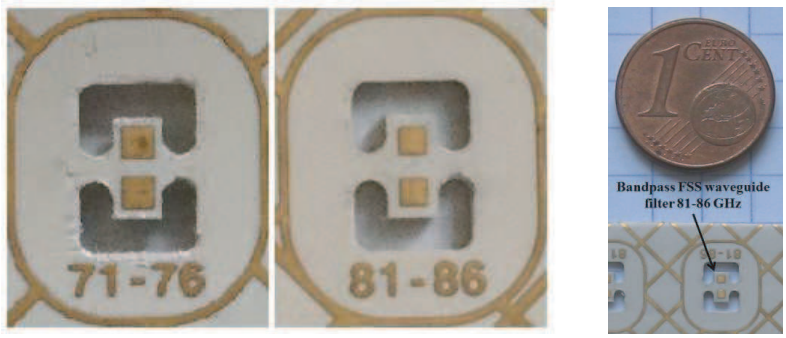

Figure 7. Photograph of the fabricated FSS waveguide band-pass filters (for the two channels: 71–76 GHz and 81–86 GHz) (Component size is compared to one cent Euro).

Based on WR90 rectangular waveguide, a fifth order, "Tchebychev" type, 0.1 dB ripple, with a relative bandwidth of about $\approx 5\%$ FSS-WBPF is designed and fabricated in the X band frequency range (around 10 GHz). The dimensions of the WR90 waveguide are 22.86 mm × 10.16 mm.

The dielectric substrate available in the laboratory is FR4. Table 3 summaries the parameters and geometric dimensions of the designed fifth order FSS WBPF.

Table 3. Parameter values of fifth order "Tchebychev" band-pass filter with a ripple of 0.1 dB and the dimensions of fabricated WR90 FSS waveguide band-pass filter around 10 GHz (9.75–10.25 GHz).

Ripple	BW	$S_1 = S_5$	$S_2 = S_3 = S_4$
0.1 dB	$\approx 5\%$	3.83 mm	3.94 mm
A	B	C	D
22.86 mm	10.16 mm	4.08 mm	9.43 mm

Order	$g_0 = g_6$	$g_1 = g_5$	$g_2 = g_4$	g_3
5	1	1.1468	1.3712	1.9750

5.1. X-Band FSS Prototype Filter: Fabrication Method and Measurements

Figure 8 presents the stacked layers of the designed X-band FSS WBPF. The fabrication process uses a combination of (i) double side printed circuit, (ii) single side printed circuit and (iii) dielectric material without any metallization. All those layers are bonded using adhesives films with different thicknesses and having a permittivity similar to that of FR4. The used bonding films are 2116, 1080, and 7268 [20]. The overall thickness of fabricated FSS filter is about $0.21\lambda \approx 6.394$ mm.

5.2. Measurement and Comparison

Figure 9 presents the fabricated prototype in the X-band frequency range. The multilayer FSS filter is inserted inside a rectangular WR90 X-band waveguide. The structure is characterized using the measurement facility of our Laboratory. A waveguide TRL calibration is performed before all the measurements using a network analyzer "Anritsu" at frequency ranging from 8 GHz to 12 GHz.

Figure 10 gives a comparison between the simulated and measured results of the designed filter. A very good agreement is observed between the HFSS simulation and the measurement results for both transmission and reflection coefficients. The magnitude of the reflection coefficient is ≈ -20 dB over the whole filter bandwidth. The insertion loss is 10 dB due to the multilayer (more than 15 layers) FR4 and bonding films dielectric loss and conductor loss. In the simulation, we take into account for the tangent loss of each layer.

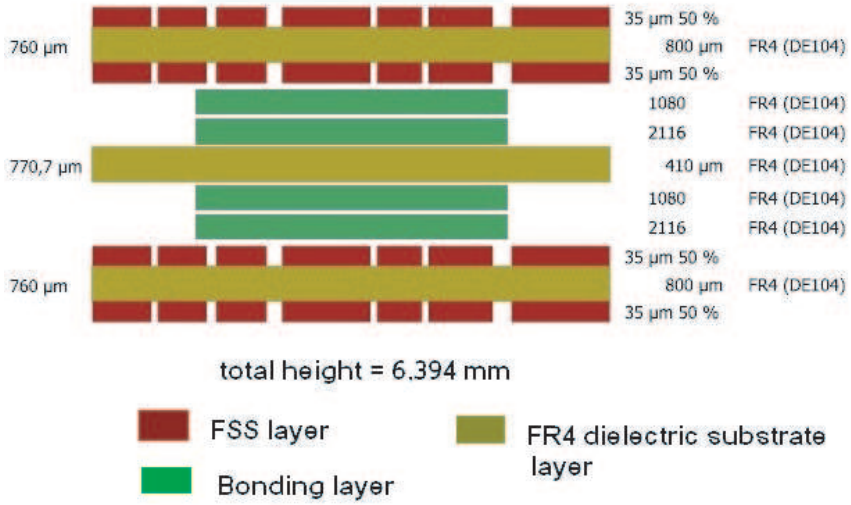

Figure 8. FSS waveguide band-pass filter bonding method: side view of different layers of the physical FSS filters structure, cascading method and bonding technique. Epoxy FR4 (double layer and single layer) and bonding films (7628, 2080, and 2116) are used.

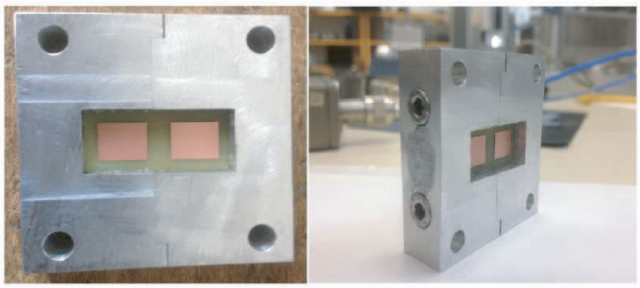

(a) (b)

Figure 9. Photograph of the fabricated FSS waveguide bandpass filter in X-band frequency range: (a) Front view. (b) Side view.

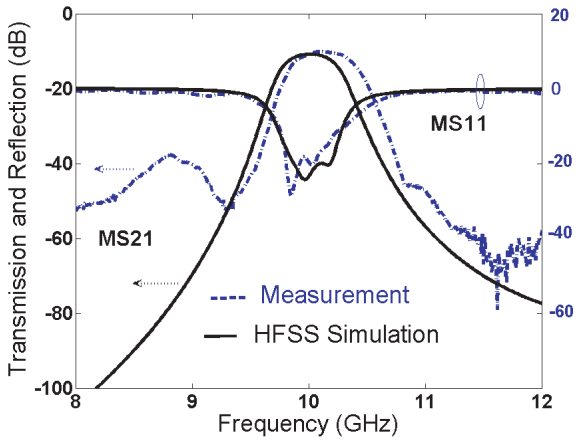

Figure 10. Comparison of HFSS simulation results and measurement results of fabricated FSS waveguide bandpass filter at X band frequency range (around 10 GHz), a good agreement between HFSS simulation results and measured results is obtained.

6. CONCLUSION

This paper presents the design and numerical study of mm-wave low-profile multilayer FSS waveguide bandpass filters with high rejection of out of band. The compact filters (thickness of $\lambda/4$) were designed for two channels, respectively 71–76 and 81–86 GHz (E-band) and inserted symmetrically in the WR12 diplexer waveguide T-junction.

The diplexer is one of the key components designed for high capacity and high-speed E-band point to point wireless communication system application (ELHAN project of the French Systematic cluster). To achieve high channel isolation (≈ 70 dB) and high rejection of out of band, a seventh-order and 13 FSS layers were required for each filter. Several prototypes of the two FSS filters have been manufactured by "ELVIA" using Rogers Ultralam 3850 (Liquid Crystalline Polymer (LCP)) dielectric material. Experimental measurements have not been made, since no measurement facilities are available in the mm-wave frequency range. The experimental validation is done in X-band (laboratory available instrumentation) by developing a fifth order FSS waveguide bandpass filter with the same procedure and design methodology. The very good agreement, obtained between the measurement and simulations, constitutes a validation of the design methodology. The proposed multilayer FSS filters and diplexer are low profile, compact and can be efficiently integrated in the future E-band millimeter-wave transceiver.

ACKNOWLEDGMENT

The authors would like to thank the Region Ile de France for its financial support for the "ELHAN" project of the Systematic French Cluster. Thanks are also given to RFS Trignac France for their collaboration, ELVIA for the manufacture of FSS waveguide band-pass prototypes at the E band frequency range, and our colleagues, Dr. Xiaoke Han, Dr. Mamadou Gueye, and Prof. Alain Priou for their help during this study.

REFERENCES

1. http://www.systematic-paris-region.org/en/projets/elhan.
2. Tang, H. J., W. Hong, J.-X. Chen, G. Q. Luo, and K. Wu, "Development of millimeter-wave planar diplexers based on complementary characters of dual-mode substrate integrated waveguide filters with circular and elliptic cavities," *IEEE Transactions on Microwave Theory and Techniques*, Vol. 55, No. 4, 776–782, April 2007.
3. Morini, A. and T. Rozzi, "Analysis of compact E-plane diplexers in rectangular waveguide," *IEEE Transactions on Microwave Theory and Techniques*, Vol. 43, No. 8, 1834–839, 1995.
4. Athanasopoulos, N. and K. Voudouris, "Development of a 60 GHz Substrate integrated waveguide planar diplexer," *IEEE MTT-S International Microwave Workshop Series on Millimeter Wave Integration Technologies*, 128–131, Barcelona, Spain, 2011.
5. Ohira, M., H. Deguchi, and M. Tsuji, "Circuit synthesis for compact waveguide filters with closely-spaced frequency selective surfaces," *International Journal of Microwave and Optical Technology*, Vol. 1, No. 2, 366–370, August 2006.
6. Cai, S.-F., Q.-Y. Wang, Z.-Y. Wang, and Y.-F. Zhai, "Design of a FSS waveguide filter at 8.05 GHz," *IEEE MTT-S International Microwave Workshop Series on Art of Miniaturizing RF and Microwave Passive Component*, 173–175, Chengdu, China, December 14–15, 2008.
7. Tsuji, M., H. Deguchi, and M. Ohira, "A new frequency selective window for constructing waveguide bandpass filters with multiple attenuation poles," *Progress In Electromagnetics Research C*, Vol. 20, 139–153, 2011.
8. Teo, P. T., K. S. Lee, and C. K. Lee, "Analysis and design of band-pass frequency-selective surfaces using the FEM CAD tool," *International Journal of RF and Microwave Computer-Aided Engineering*, Vol. 14, No. 5, 391–397, September 2004.
9. Munk, B. A., *Frequency Selective Surfaces Theory and Design*, Wiley-Interscience John Wiley & Sons, Inc., 2000.

10. Sarabandi, K. and N. Behdad, "A frequency selective surface with miniaturized elements," *IEEE Transactions on Antennas and Propagation*, Vol. 55, No. 5, 1239–1245, May 2007.
11. Al-Joumayly, M. and N. Behdad, "A new technique for design of low-profile, second-order, bandpass frequency selective surfaces," *IEEE Transactions on Antennas and Propagation*, Vol. 57, No. 2, 452–459, 2009.
12. Behdad, N. and M. Al-Joumayly, "A generalized method for synthesizing low-profile, band-pass frequency selective surfaces with non-resonant constituting elements," *IEEE Transactions on Antennas and Propagation*, Vol. 58, No. 12, 4033–4041, December 2010.
13. Zhang, T., H. H. Ouslimani., Y. Letestu, A. Le Bayon, and L. Renard Darvil, "A low profile multilayer seventh order band-pass frequency selective surface (FSS) for millimeter-wave application," *IEEE 13th, Annual Wireless and Microwave Technology Conference: IEEE Industry/Government/Education Conf. (WAMICON)*, Cocoa Beach, USA, 2012.
14. Behdad, N. and M. Al-Joumayly, "A generalized synthesis procedure for low-profile, frequency selective surfaces with odd-order bandpass responses," *IEEE Transactions on Antennas and Propagation*, Vol. 58, No. 7, 2460–2464, 2010.
15. Behdad, N., M. Al-Joumayly, and M. Salehi, "A low-profile third-order bandpass frequency selective surface," *IEEE Transactions on Antennas and Propagation*, Vol. 57, No. 2, 460–466, 2009.
16. Collin, R. E., *Foundations for Microwave Engineering*, John Wiley & Sons, Inc., 2001.
17. George L., L. Y. Matthaei, E. M. T. Jones, *Microwave Filters, Impedance-matching Networks, and Coupling Structures*, Artech House, Inc., 1980.
18. Marcuvitz, N., *Waveguide Handbook*, Inspec/IEE., Vol. 448, 1986.